

Linear seesaw mechanism from dark sector

A. E. Cárcamo Hernández,^{1,2,3,*} Vishnudath K. N.,^{1,†} and José W. F. Valle^{4,‡}

¹*Universidad Técnica Federico Santa María, Casilla 110-V, Valparaíso, Chile*

²*Centro Científico-Tecnológico de Valparaíso, Casilla 110-V, Valparaíso, Chile*

³*Millennium Institute for Subatomic Physics at High-Energy Frontier (SAPHIR), Fernández Concha 700, Santiago, Chile*

⁴*AHEP Group, Institut de Física Corpuscular – CSIC/Universitat de València, Parc Científic de Paterna.
C/ Catedrático José Beltrán, 2 E-46980 Paterna (Valencia) - SPAIN*

We propose a minimal model where a dark sector seeds neutrino mass generation radiatively within the linear seesaw mechanism. Neutrino masses are calculable, since tree-level contributions are forbidden by symmetry. They arise from spontaneous lepton number violation by a small Higgs triplet vacuum expectation value. Lepton flavour violating processes e.g. $\mu \rightarrow e\gamma$ can be sizeable, despite the tiny neutrino masses. We comment also on dark-matter and collider implications.

I. INTRODUCTION

Two solid indications for new physics beyond the Standard Model (SM) are the existence of neutrino masses [1, 2] and dark matter [3]. There are many ways to induce neutrino masses, and at the moment we do not know which one is nature’s choice. There are also many options to add new electrically neutral fermions and/or scalars to the SM so as to provide a viable dark matter (DM) candidate. Typically the latter is made stable through the imposition of an adequate “dark parity” symmetry.

In most of these SM extensions there is no relation between dark matter and neutrino mass generation. There has been a recent suggestion that neutrino mass generation proceeds *a la seesaw* within the $SU(3)_c \otimes SU(2)_L \otimes U(1)_Y$ framework [4, 5], seeded by a dark sector [6–11]¹. This way neutrino mass generation becomes intimately connected with dark matter physics.

In this paper we suggest that neutrino masses are seeded by a dark sector within the context of the linear seesaw mechanism [24–26]. Several SM extensions implementing the linear seesaw mechanism have been used recently to approach the flavor problem [27–29]. Here we focus on the dark matter issue, proposing a dark-seeded linear seesaw mechanism, as an alternative to the dark-seeded extension of the inverse seesaw [30, 31]. This new realization makes use of the simplest template structure shared by all low-scale seesaw schemes, and employs a very simple dark sector. The latter consists of one SM doublet and a singlet dark scalar, while for dark fermions we employ three SM singlet two-component Majorana fermions. The Higgs sector contains, besides the SM doublet, a complex isotriplet involved in seeding neutrino mass generation.

Many phenomenological implications of our proposal are also expected in generic linear seesaw setups [32, 33]. Besides these, we have a Weakly Interacting Massive Particle (WIMP) dark-matter candidate, that can be identified with the lightest electrically neutral dark particle (LDP). Rather than being associated to supersymmetry [34], WIMP dark-matter emerges here as a neutrino mass mediator, in a manner distinct from scotogenic approaches [35, 36], and also inequivalent to the dark inverse-seesaw realization [10]. We examine the most salient phenomenological implications of the dark linear seesaw mechanism, concerning charged lepton flavor violation, and comment also on dark matter and collider physics implications.

* antonio.carcamo@usm.cl

† vishnudath.neelakand@usm.cl

‡ valle@ific.uv.es

¹ Low-scale seesaw schemes have been investigated extensively in recent years [12–14]. In particular, radiative constructions implementing, e.g., supersymmetry, extended gauge and/or family symmetries have been proposed, see [15–23].

II. THE MODEL

Our proposed model can be seen as a minimal extension of the inert doublet model where the linear seesaw mechanism producing the tiny neutrino masses is implemented at the one-loop level, seeded by the dark sector. The SM lepton sector is enlarged by the inclusion of the neutral leptons N_i^c and S_i ($i = 1, 2, 3$), characteristic of low-scale seesaw schemes. The dark sector contains three copies of SM singlet two-component Majorana fermions F_i , plus a SM doublet dark scalar η , and a dark gauge singlet ξ . These dark scalars η and ξ and the dark fermions F_i seed linear-seesaw neutrino mass generation as seen in Fig 1. The $SU(3)_c \otimes SU(2)_L \otimes U(1)_Y$ gauge symmetry is supplemented by the inclusion of the global $U(1)_\mathcal{L}$ lepton number symmetry, which spontaneously breaks to a preserved \mathcal{Z}_2 symmetry. This remnant symmetry, which can be identified as the matter parity $(-1)^{3\mathcal{B}+\mathcal{L}+2s}$ with \mathcal{B} , \mathcal{L} and s being the baryon, lepton and spin quantum numbers respectively, ensures the stability of the dark matter candidate, as well as the radiative nature of neutrino mass generation through the linear seesaw mechanism.

The scalar sector of our model also requires Higgs bosons to drive spontaneous breaking of the gauge and global symmetries. Besides the SM doublet Φ , we include a complex scalar isotriplet Ξ whose vacuum expectation value (VEV) is restricted by precision electroweak measurements, i.e. the ρ parameter [37]. The leptons and scalars of the model and their transformation properties under the $SU(3)_c \otimes SU(2)_L \otimes U(1)_Y$ gauge symmetry, the global lepton number symmetry, and the remnant \mathcal{Z}_2 symmetry are given in Table. I.

	L_i	l_i^c	N_i^c	S_i	Φ	Ξ	F_i	η	ξ
$SU(2)_L \times U(1)_Y$	$(2, -\frac{1}{2})$	$(1, 1)$	$(1, 0)$	$(1, 0)$	$(2, \frac{1}{2})$	$(3, 0)$	$(1, 0)$	$(2, \frac{1}{2})$	$(1, 0)$
$U(1)_\mathcal{L}$	1	-1	-1	1	0	2	0	-1	-1
$(-1)^{3\mathcal{B}+\mathcal{L}+2s}$	1	1	1	1	1	1	-1	-1	-1

TABLE I: Fields and their quantum numbers. All fermions come in three copies, $i = 1, 2, 3$.

Notice that the leptons have the conventional lepton number assignment characteristic of low-scale seesaw schemes. Together with the dark scalars, the new Majorana neutral fermions F_i play a key role in seeding non-zero neutrino masses. Except for the SM scalar doublet Φ , all scalars carry non-zero lepton number. The relevant neutrino Yukawa couplings and mass terms invariant under these symmetries are,

$$\begin{aligned}
-\mathcal{L}_Y^{(\nu)} = & \sum_{i,j=1}^3 Y_{ij}^{(\Phi)} L_i^T C N_j^c \Phi + \sum_{i,j=1}^3 Y_{ij}^{(\eta)} L_i^T C F_j \eta + \sum_{i,j=1}^3 Y_{ij}^{(\xi)} S_i^T C F_j \xi \\
& + \sum_{i=1}^3 (m_F)_i F_i^T C F_i + \sum_{i,j=1}^3 M_{ij} N_i^{cT} C S_j + \sum_{i,j=1}^3 Y'_{ij}^{(\xi)} F_i^T C N_j^c \xi^* + H.c.
\end{aligned} \tag{1}$$

The scalar potential contains,

$$\begin{aligned}
\mathcal{V}_{(s)} = & -\mu_\Phi^2 (\Phi^\dagger \Phi) - \mu_\Xi^2 Tr(\Xi^\dagger \Xi) + \mu_\eta^2 (\eta^\dagger \eta) + \mu_\xi^2 (\xi^* \xi) + A_\Phi (\Phi^\dagger \Xi \Phi + \Phi^\dagger \Xi^\dagger \Phi) \\
& + \lambda_1 (\Phi^\dagger \Phi)^2 + \lambda_2 (\eta^\dagger \eta)^2 + \lambda_3 (\xi^* \xi)^2 + \lambda_4 [Tr(\Xi^\dagger \Xi)]^2 + \lambda_5 Tr[(\Xi^\dagger \Xi)^2] \\
& + \lambda_6 (\Phi^\dagger \Phi)(\eta^\dagger \eta) + \lambda_7 (\Phi^\dagger \eta)(\eta^\dagger \Phi) + \lambda_8 (\Phi^\dagger \Phi) Tr(\Xi^\dagger \Xi) + \lambda_9 \Phi^\dagger \Xi \Xi^\dagger \Phi \\
& + \lambda_{10} (\Phi^\dagger \Phi)(\xi^* \xi) + \lambda_{11} (\eta^\dagger \eta) Tr(\Xi^\dagger \Xi) + \lambda_{12} \eta^\dagger \Xi \Xi^\dagger \eta + \lambda_{13} (\eta^\dagger \eta)(\xi^* \xi) \\
& + \lambda_{14} (\xi^* \xi) Tr(\Xi^\dagger \Xi) + \lambda_{15} (\eta^\dagger \Xi^* \Phi \xi^* + h.c.).
\end{aligned} \tag{2}$$

The $U(1)_\mathcal{L}$ symmetry is broken by the VEV of the neutral part of Ξ . The presence of the trilinear term A_Φ in Eq. (2) also breaks the global $U(1)_\mathcal{L}$ symmetry of Eqn. (1), explicitly but softly. Dark matter stability is ensured by the remnant unbroken \mathcal{Z}_2 symmetry preserved after the breaking of the $U(1)_\mathcal{L}$ symmetry. To ensure this we require that the \mathcal{Z}_2 -odd scalars η and ξ do not acquire vacuum expectation values.

The scalar fields Φ , Ξ , η and ξ can be written as follows,

$$\begin{aligned}\Phi &= \begin{pmatrix} \phi^+ \\ \frac{v_\Phi + \phi_R^0 + i\phi_I^0}{\sqrt{2}} \end{pmatrix}, & \eta &= \begin{pmatrix} \eta^+ \\ \frac{\eta_R^0 + i\eta_I^0}{\sqrt{2}} \end{pmatrix}, \\ \Xi &= \begin{pmatrix} \frac{v_\Xi + \Xi_R^0 + i\Xi_I^0}{\sqrt{2}} & \Xi_1^+ \\ \Xi_2^- & -\frac{v_\Xi + \Xi_R^0 + i\Xi_I^0}{\sqrt{2}} \end{pmatrix}, & \xi &= \frac{\xi_R + i\xi_I}{\sqrt{2}}.\end{aligned}$$

We have two charged Higgs scalars Ξ_1^\pm and Ξ_2^\pm with mass-squared given as,

$$m_{\Xi_{1,2}^\pm}^2 = \frac{\sqrt{2}A_\Phi(v_\Phi^2 + 4v_\Xi^2) \mp \sqrt{32A_\Phi^2 v_\Xi^4 + v_\Phi^2 v_\Xi^2(v_\Phi^2 + 8v_\Xi^2)\lambda_9^2}}{4v_\Xi}, \quad (3)$$

and a charged dark scalar η^\pm with mass-squared given as,

$$m_{\eta^\pm}^2 = \frac{1}{2}v_\Xi^2(2\lambda_{11} + \lambda_{12}) + \frac{1}{2}v_\Phi^2\lambda_6 + \mu_\eta^2. \quad (4)$$

We also note that, in the presence of the cubic term A_Φ the two charged components of the triplet scalar will have an adequate mass-squared term.

Electroweak symmetry breaking is driven mainly by the VEV of Φ . The resulting mass squared matrices for the CP-even neutral Higgs scalars are given as,

$$M_{\phi_R^0 \Xi_R^0}^2 = \begin{pmatrix} 2\lambda_1 v_\Phi^2 & v_\Phi(-\sqrt{2}A_\Phi + v_\Xi(2\lambda_8 + \lambda_9)) \\ v_\Phi(-\sqrt{2}A_\Phi + v_\Xi(2\lambda_8 + \lambda_9)) & \frac{A_\Phi v_\Phi^2}{\sqrt{2}v_\Xi} + 4v_\Xi^2(2\lambda_4 + \lambda_5) \end{pmatrix}, \quad (5)$$

while the corresponding neutral dark scalar mass squared matrices are given as,

$$M_{\eta_R^0 \xi_R}^2 = \begin{pmatrix} \frac{v_\Xi^2}{2}(2\lambda_{11} + \lambda_{12}) + \frac{v_\Phi^2}{2}(\lambda_6 + \lambda_7) + \mu_\eta^2 & -\frac{1}{2}\lambda_{15}v_\Phi v_\Xi \\ -\frac{1}{2}\lambda_{15}v_\Phi v_\Xi & \frac{1}{2}\lambda_{10}v_\Phi^2 + \lambda_{14}v_\Xi^2 + \mu_\xi^2 \end{pmatrix}, \quad (6)$$

$$M_{\eta_I^0 \xi_I}^2 = \begin{pmatrix} \frac{v_\Xi^2}{2}(2\lambda_{11} + \lambda_{12}) + \frac{v_\Phi^2}{2}(\lambda_6 + \lambda_7) + \mu_\eta^2 & \frac{1}{2}\lambda_{15}v_\Phi v_\Xi \\ \frac{1}{2}\lambda_{15}v_\Phi v_\Xi & \frac{1}{2}\lambda_{10}v_\Phi^2 + \lambda_{14}v_\Xi^2 + \mu_\xi^2 \end{pmatrix}. \quad (7)$$

There is also a CP-odd scalar coming from the imaginary part of the neutral component of Ξ , whose mass is given as,

$$m_{\Xi^0 I}^2 = \frac{A_\Phi v_\Phi^2}{\sqrt{2}v_\Xi}. \quad (8)$$

Thus, one sees that the physical scalar spectrum includes four CP-even scalars: two neutral Higgs H_1 and H_2 arising from the mixing of Ξ_R^0 and ϕ_R^0 , and containing the 125 GeV SM Higgs boson [38, 39], plus two dark neutral scalars D_1 and D_2 arising from the mixing of η_R^0 and ξ_R . Moreover, we have two dark neutral CP-odd scalars, D_{A_1} and D_{A_2} arising from the mixing of η_I^0 and ξ_I and another CP-odd scalar corresponding to $\Xi^0 I$. The doublet-singlet mixing angles in these matrices are expected to be naturally small, thanks to the limit $v_\Xi \lesssim 3\text{GeV}$ from the ρ parameter.

Note also that, thanks to the cubic lepton number soft-breaking term A_Φ present in Eq. (2), all physical scalars are massive. This avoids the existence of a Majoron [5, 40], a physical Nambu-Goldstone boson associated to spontaneous lepton number violation. This gets an adequately large mass from the explicit A_Φ -induced breaking of lepton number. An alternative full-fledged Majoron scheme can also be implemented, along the lines of Ref. [41]. However we do not pursue such extension here, as it is not essential for the neutrino mass generation.

We now turn to the radiative neutrino mass generation via linear seesaw mechanism. The lepton Yukawa interactions yield the following neutrino mass terms,

$$-\mathcal{L}_{mass}^{(\nu)} = \frac{1}{2} \begin{pmatrix} \nu^T & N^{cT} & S^T \end{pmatrix} M_\nu C \begin{pmatrix} \nu \\ N^c \\ S \end{pmatrix} + H.c., \quad (9)$$

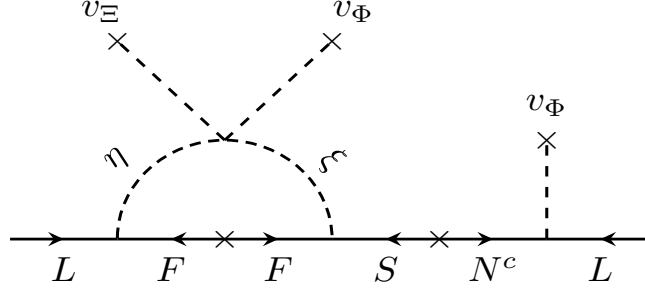


FIG. 1: Feynman diagram for neutrino mass generation in dark linear seesaw mechanism (plus symmetrization).

where the neutrino mass matrix M_ν is given as,

$$M_\nu = \begin{pmatrix} 0_{3 \times 3} & m_D & \varepsilon \\ m_D^T & 0_{3 \times 3} & M \\ \varepsilon^T & M & 0_{3 \times 3} \end{pmatrix}. \quad (10)$$

Here the submatrix M is a bare mass, and m_D is generated at tree-level after electroweak symmetry breaking,

$$m_D = Y^{(\Phi)} \frac{v_\Phi}{\sqrt{2}}. \quad (11)$$

In contrast, the small entry ε arises radiatively, mediated by the one-loop level exchange of the dark fermions and scalars. The one-loop level Feynman diagram is given in Fig. 1 and the resulting submatrix ε is given as,

$$\varepsilon_{ij} = \sum_{k=1}^3 \frac{Y_{ik}^{(\eta)} Y_{jk}^{(\xi)} M_{F_k}}{16\pi^2} \left\{ [f(m_{D_1}^2, m_{F_k}^2) - f(m_{D_2}^2, m_{F_k}^2)] \sin 2\theta_D - [f(m_{D_{A_1}}^2, m_{F_k}^2) - f(m_{D_{A_2}}^2, m_{F_k}^2)] \sin 2\theta_{D_A} \right\}, \quad (12)$$

where $f(m_1, m_2)$ is the function defined as,

$$f(m_1, m_2) = \frac{m_1^2}{m_1^2 - m_2^2} \ln \left(\frac{m_1^2}{m_2^2} \right). \quad (13)$$

Here m_{D_1} and m_{D_2} are the masses of the physical CP even dark scalars, whereas $m_{D_{A_1}}$ and $m_{D_{A_2}}$ are those that of the dark pseudoscalars. Their mixing matrices are defined as,

$$\begin{pmatrix} D_1 \\ D_2 \end{pmatrix} = \begin{pmatrix} \cos \theta_D & \sin \theta_D \\ -\sin \theta_D & \cos \theta_D \end{pmatrix} \begin{pmatrix} \eta_R \\ \xi_R \end{pmatrix}, \quad \begin{pmatrix} D_{A_1} \\ D_{A_2} \end{pmatrix} = \begin{pmatrix} \cos \theta_{D_A} & \sin \theta_{D_A} \\ -\sin \theta_{D_A} & \cos \theta_{D_A} \end{pmatrix} \begin{pmatrix} \eta_I \\ \xi_I \end{pmatrix}. \quad (14)$$

where the small doublet-singlet mixing angles θ_D and θ_{D_A} are obtained by diagonalizing Eqns. (6) and (7), respectively, from which one sees $\theta_{D_A} = -\theta_A$.

Given a non-zero submatrix ε , the light active neutrino masses arise from the linear seesaw mechanism [24–26], so that the resulting active-neutrino mass matrix has the form,

$$m_{\text{light}} = -[m_D M^{-1} \varepsilon^T + \varepsilon M^{-1} m_D^T]. \quad (15)$$

One sees that spontaneous lepton number violation through v_Ξ provides a radiative seed for light neutrino mass generation that proceeds *a la seesaw*. The smallness of the light neutrino masses is ascribed to the smallness of loop-suppressed ε as well as the small, but not necessarily negligible, $\frac{m_D}{M}$ ratio. It is worth mentioning that small neutrino masses are symmetry-protected, making the model natural in t'Hooft's sense.

On the other hand, as in all low-scale seesaw models, our heavy mediator neutrino sector consists of three pairs of quasi-Dirac [42–44] heavy neutrinos, whose mass matrices are given as,

$$M_{N^-} = -M - m_D^T m_D M^{-1} + \frac{1}{2} [m_D M^{-1} \varepsilon^T + \varepsilon M^{-1} m_D^T], \quad (16)$$

$$M_{N^+} = M + m_D^T m_D M^{-1} + \frac{1}{2} [m_D M^{-1} \varepsilon^T + \varepsilon M^{-1} m_D^T]. \quad (17)$$

III. PHENOMENOLOGY

A. Charged lepton flavor violation

In this section we discuss the implications of our model for charged lepton flavor violation (cLFV). In particular, we focus on the radiative decays $\ell_i \rightarrow \ell_j \gamma$, the most sensitive of which is the decay $\mu \rightarrow e \gamma$. A key conceptual feature of low-scale seesaw, such as our proposed dark linear seesaw-scheme, is that leptonic flavour and CP can be violated even in the limit of massless neutrinos [45–48]. That means that the cLFV rates are not suppressed by the small neutrino masses, and can therefore be sizeable.

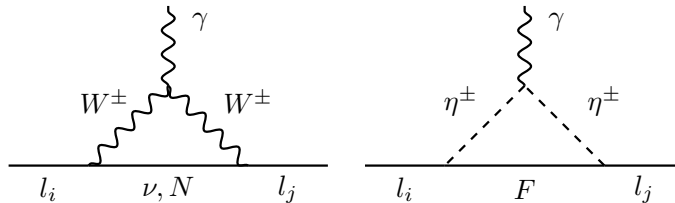


FIG. 2: Feynman diagrams that contribute to $l_i \rightarrow l_j \gamma$ processes. The left diagram shows the charged-current contribution, whereas the one in the right shows the dark-sector contribution.

In the same spirit as [49] one can give an approximate expression for extracting the “Dirac” submatrix in terms of the measured oscillation parameters as follows [50, 51],

$$m_D = U_{lep} \sqrt{m_\nu} A^T \sqrt{m_\nu} U_{lep}^T (\varepsilon^T)^{-1} M^T, \quad \text{with} \quad A = \begin{pmatrix} \frac{1}{2} & a & b \\ -a & \frac{1}{2} & c \\ -b & -c & \frac{1}{2} \end{pmatrix}, \quad (18)$$

where a , b and c are taken to be real numbers, $m_\nu = \text{diag}(m_1, m_2, m_3)$ is given by the light neutrino masses, and U_{lep} is approximately the lepton mixing matrix determined in oscillation experiments [52]. We assume the basis in which the charged lepton mass matrix is diagonal. From this expression it is clear that, given m_ν from oscillation measurements, one can fix m_D in accordance with the corresponding mass scale ratio ε/M so as to fit the oscillations. Likewise, concerning mixing parameters, one can choose the off-diagonal entries of m_D to match the measured solar, atmospheric and reactor mixing angles. In fact, taking as a simple ansatz M and ε diagonal and proportional to identity, one sees that m_{Dij} can be chosen so as to fit the observed mixing angles.

The $\mu \rightarrow e \gamma$ decay amplitude involves the Feynman diagrams in Fig. 2. There are two types of contributions, i.e. the charged-current (CC) contribution (left diagram) and a contribution arising from the dark sector (right diagram). In order to determine the CC contribution the key ingredient is the full lepton mixing matrix, which has a rectangular form [4, 5]. Such rectangular mixing matrix describes not only the CC couplings of the light neutrinos, which gives a sizeable contribution due to the effective unitarity violation, of order $(\frac{m_D}{M})^2$, but also the heavy mediator neutrino admixture in the left-handed CC weak interaction, of order $(\frac{m_D}{M})$. We find that the CC light-neutrino contribution to the $\mu \rightarrow e \gamma$ decay can be sizeable, thanks to effective unitarity violation of the relevant coupling sub-matrix. Moreover, one has potentially large contributions also due to the exchange of the six sub-dominantly coupled heavy quasi-Dirac states, that can lie at the TeV scale, or even lower.

In our dark linear seesaw, charged lepton flavor violation can also be mediated by the charged scalar η^\pm and the dark fermions F_i through the couplings $Y^{(\eta)}$, as shown in Fig. 2. This second contribution is especially interesting as the same dark sector Yukawa couplings $Y^{(\eta)}$ generating neutrino masses radiatively via the linear seesaw can also give rise to charged lepton flavor violation. The Feynman diagrams for these two contributions are shown in Fig. 2.

The total branching ratio for the process $\mu \rightarrow e\gamma$ thus takes the form [46, 53, 54],

$$Br(\mu \rightarrow e\gamma) = \frac{3(4\pi)\alpha_{em}}{4G_F^2} \left| \sqrt{\frac{\alpha_W^2 s_W}{m_W^4}} \sum_{k=1}^9 K_{2k}^* K_{1k} G_F \left(\frac{M_k^2}{m_W^2} \right) + \sum_{k=1}^3 \frac{Y_{2k}^{(\eta)} Y_{2k}^{(\eta)}}{2m_{\eta^\pm}^2} G_{\eta^\pm} \left(\frac{m_{F_k}^2}{m_{\eta^\pm}^2} \right) \right|^2, \quad (19)$$

with,

$$G_F(x) = \frac{10 - 43x + 78x^2 - 49x^3 + 18x^3 \ln x + 4x^4}{12(1-x)^4}, \quad (20)$$

$$G_{\eta^\pm}(x) = \frac{1 - 6x + 3x^2 + 2x^3 - 6x^2 \ln x}{6(1-x)^4}. \quad (21)$$

In Eqn. (19), the matrix K is the 3×9 rectangular mixing matrix describing the CC weak interaction and includes the exchange of the three light active neutrinos with $k = 1, 2, 3$ as well as the six mediators, with $k = 4, 5, \dots, 9$. As mentioned earlier these form three quasi-Dirac heavy-neutrino pairs.

The complete form of the lepton mixing matrix K is given by:

$$K = (K_L, K_H), \quad (22)$$

where K_L and K_H are 3×3 and 3×6 matrices, respectively. These submatrices take the form:

$$K_L = \left(1_{3 \times 3} - \frac{1}{2} m_D (M^{-1})^T M^{-1} m_D^\dagger \right) U_{lep} = \left(1_{3 \times 3} - \frac{1}{2} V V^\dagger \right) U_{lep}, \quad (23)$$

$$K_H = \left(-\frac{i}{\sqrt{2}} V, \frac{1}{\sqrt{2}} V \right), \quad V = m_D (M^{-1})^T. \quad (24)$$

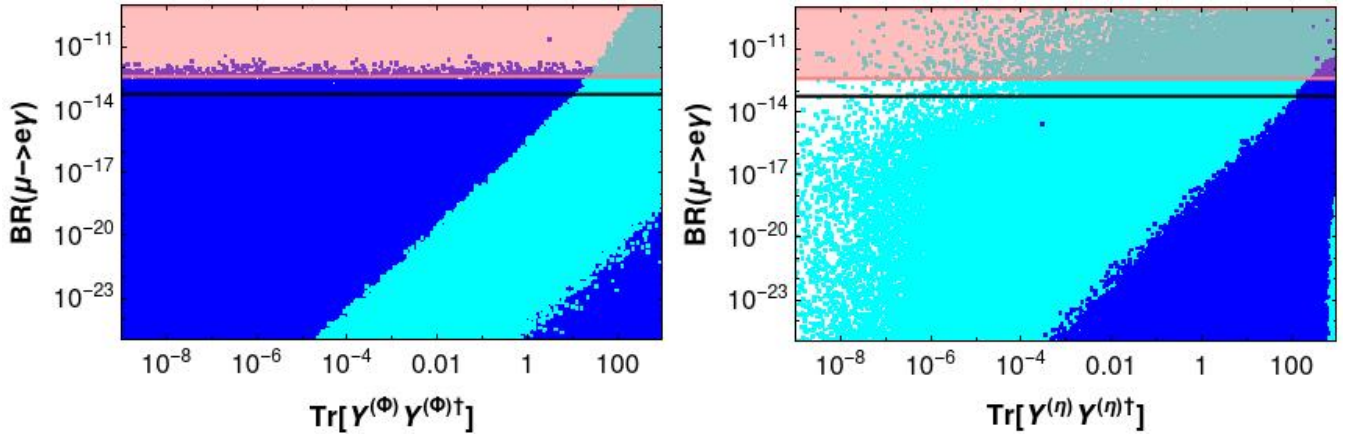


FIG. 3: Correlations of $Br(\mu \rightarrow e\gamma)$ against the $\text{Tr}[Y^{(\Phi)} Y^{(\Phi)\dagger}]$ and $\text{Tr}[Y^{(\eta)} Y^{(\eta)\dagger}]$. The cyan points correspond to the CC contribution, whereas the blue points show the dark-sector contribution.

Parameters	Y_{ij}^η	$Y_{ij}^\xi = y\delta_{ij}$	m_{F_i}	$M_{ij} = M_N \delta_{ij}$	$m_{D_1, D_2, D_{A_1}, D_{A_2}, \eta^\pm}$	θ_D	a, b, c
Range	$[10^{-10}, 4\pi]$	$[10^{-16}, 4\pi]$	$[200, 5000]$ GeV	$[200, 5000]$ GeV	$[200, 5000]$ GeV	0.01	$[-20, 20]$

TABLE II: The sampling region used in generating the plots of Fig. 3.

In Fig. 3, we present the correlations of $Br(\mu \rightarrow e\gamma)$ against $\text{Tr}[Y^{(\Phi)} Y^{(\Phi)\dagger}]$ (left) and $\text{Tr}[Y^{(\eta)} Y^{(\eta)\dagger}]$ (right). In order to optimize our parameter scan to generate these figures, ensuring that only viable solutions consistent with

neutrino oscillation data are included, it is useful to use the analytical approximation in Eq. (18). Note however, that in presenting the numerical results we use the exact expressions for the diagonalization matrices.

In generating Fig. 3, the neutrino oscillation parameters are varied in their 3σ ranges [52], the parameters a , b and c are varied in the range $[-20, 20]$ and the couplings $Y_{ij}^{(\eta)}$ are varied up to 4π . For simplicity we took the heavy neutrinos as degenerate, varying their masses in the range $[200, 5000]$ GeV. Concerning the dark sector parameters, $Y_{ij}^{(\xi)}$ is taken as $y\delta_{ij}$ with y varied up to 4π . The masses of the dark fermions F_i and the scalar masses are varied in the range $[200, 5000]$ GeV, while the scalar mixing angle θ_D is fixed to be 0.01 implying $\theta_{D_A} = -0.01$. The sampling region is summarized in table II.

In Fig. 3, the cyan and the blue points show the CC and the dark-sector contributions to $Br(\mu \rightarrow e\gamma)$, respectively. The horizontal pink-shaded region corresponds to the current bound [55], $Br(\mu \rightarrow e\gamma) < 4.2 \times 10^{-13}$ as obtained from the MEG experiment, whereas the black line corresponds to the projected future sensitivity of 6×10^{-14} for MEG-II [56, 57]. From the expression for the branching ratio, one can see that the CC contribution depends on $Y^{(\Phi)}$, whereas the dark sector contribution depends only on $Y^{(\eta)}$. This correlation can also be seen from Fig. 3. We find that even if the CC contribution is low (in the regions of small $Y^{(\Phi)}$), for large values of $Y^{(\eta)}$ the dark sector contribution can take values as large as the existing limit. Part of this parameter space will be probed by MEG-II.

B. Dark matter phenomenology

In this section we discuss the implications of our model for dark matter. Due to the remnant \mathcal{Z}_2 symmetry arising from the spontaneous breaking of the global $U(1)_{\mathcal{L}}$ lepton number symmetry, our model will have a stable dark matter candidate, which we call the LDP.

1. Fermionic dark matter

As a warm up, we start by considering a simple scenario in which the LDP is fermionic, i.e. the lightest of the heavy Majorana fermions F_i ($i = 1, 2, 3$). It can annihilate into a pair of SM active neutrinos via the t -channel exchange of the CP-even and CP-odd parts of the neutral component of the dark scalar doublet η , as shown in the Feynman diagram of Fig. 4.

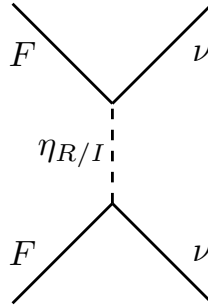


FIG. 4: Annihilation of a pair of fermionic dark matter candidates into a pair of active neutrinos.

In this case, the thermally-averaged annihilation cross section is given by [58],

$$\langle\sigma v\rangle \simeq \frac{9\left(Y_{11}^{(\eta)}\right)^4}{32\pi} \frac{m_{F_1}^2\left(2m_{F_1}^2+m_{D_1}^2+m_{D_{A_1}}^2\right)^2}{\left(m_{F_1}^2+m_{D_1}^2\right)^2\left(m_{F_1}^2+m_{D_{A_1}}^2\right)^2}, \quad (25)$$

where we have assumed F_1 to be the lightest among F_i . Here $Y_{11}^{(\eta)}$ is the Yukawa coupling with the dark scalar doublet η . From the previous relation, we find the following estimate for the DM relic abundance [37],

$$\frac{\Omega_{DM} h^2}{0.12} = \frac{0.1 pb}{0.12 \langle \sigma v \rangle} = \frac{0.1 pb}{0.12} \left[\frac{9 \left(Y_{11}^{(\eta)} \right)^4}{32\pi} \frac{m_{F_1}^2 \left(2m_{F_1}^2 + m_{D_1}^2 + m_{D_{A_1}}^2 \right)^2}{\left(m_{F_1}^2 + m_{D_1}^2 \right)^2 \left(m_{F_1}^2 + m_{D_{A_1}}^2 \right)^2} \right]^{-1}, \quad (26)$$

which in turn can reproduce the observed DM relic abundance of [59],

$$\Omega_{DM} h^2 = 0.1200 \pm 0.0012 \quad (27)$$

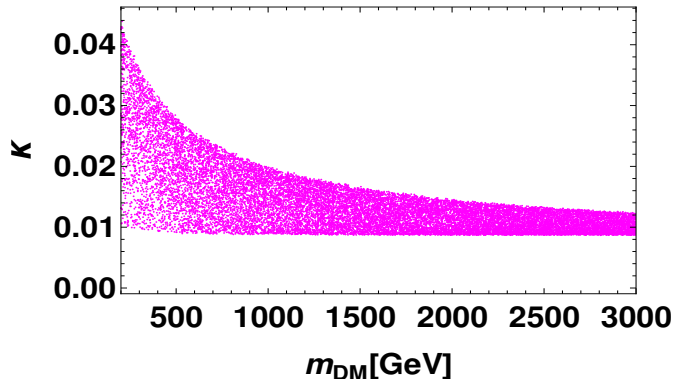


FIG. 5: Allowed region in the $m_{DM} - \kappa$ plane that reproduces the correct fermionic dark matter relic density. Here m_{DM} is the mass of the lightest dark fermion, i.e. m_{F_1} , and κ is the corresponding Yukawa coupling, $Y_{11}^{(\eta)}$.

In Fig. 5 we present the allowed parameter space in the $m_{F_1} - Y_{11}^{(\eta)}$ plane that reproduces the measured values of the dark matter relic abundance. In generating this figure, the masses of the dark scalars m_{D_1} and $m_{D_{A_1}}$ are both varied in the range 0.2-5 TeV. From the figure, one can see that the allowed range of the Yukawa couplings for lower values of the dark matter mass is broader.

However, since the fermionic dark matter F_1 couples only to the dark scalars, this scenario can not be probed by direct detection techniques based on nuclear recoil measurements. For this reason we now move to an alternative interesting scenario where one of the neutral scalars of the dark sector is the LDP, and hence the DM candidate.

2. Scalar dark matter

Scenarios with a scalar DM candidate have been well studied within the framework of generalized scotogenic or inert doublet models [36, 60–67]. This DM possibility can arise in our present model by assuming that the LDP is the lightest among the neutral scalar particles D_1 , D_2 , D_{A_1} , D_{A_2} , and lighter than the heavy neutral Majorana fermions F_i . In the following discussion, we take small doublet-singlet mixing angles so that D_{A_1} , taken as the DM candidate, is mainly the imaginary part of the neutral component of the dark doublet η . Such a scalar DM candidate would scatter off a nuclear target through Higgs boson exchange in the t -channel. This gives rise to a direct Higgs portal dark-matter detection mechanism that can be used to probe the coupling parameter characterizing the $H_1^2 D_{A_1}^2$ interaction.

We assume that the main coannihilation channels for the DM candidate lead to a pair of SM particles as well as charged and the neutral components of the scalar triplet, as shown in Fig. 6. In this benchmark scenario, we take all dark sector quartic couplings except $\lambda_{6,7,11}$ to be small. Thus, the dominant contributions to the DM coannihilation

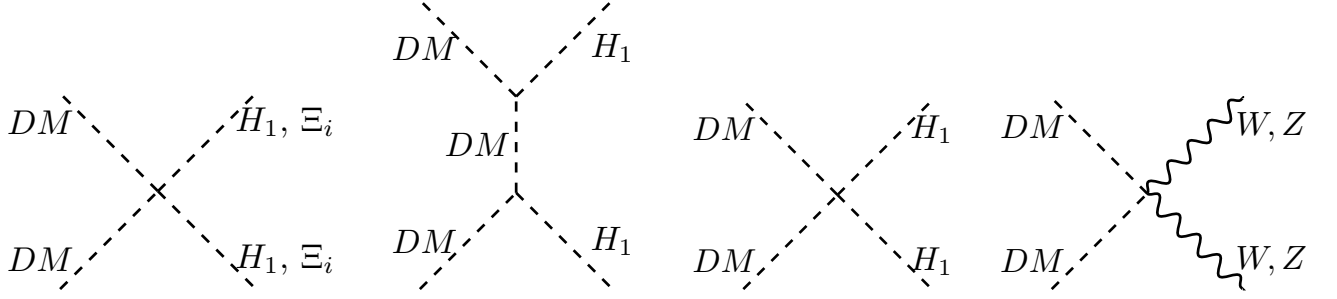


FIG. 6: Dominant Feynman diagrams contributing to dark-matter annihilation for the benchmark considered.

are shown in Fig. 6. The corresponding annihilation cross sections are given as [68, 69],

$$v_{rel}\sigma(D_{A_1}D_{A_1} \rightarrow WW) = \frac{1}{8\pi m_{DM}\sqrt{s}} \frac{g^4}{4} \left(1 + \frac{m_{DM}^4}{m_W^4} \left(\frac{\Delta m^2 + \kappa v_\Phi^2}{m_{DM}^2}\right)^2\right) \sqrt{1 - \frac{4m_W^2}{s}}, \quad (28)$$

$$v_{rel}\sigma(D_{A_1}D_{A_1} \rightarrow ZZ) = \frac{1}{16\pi m_{DM}\sqrt{s}} \frac{g^2}{4c_w^4} \left(1 + \frac{m_{DM}^4}{m_Z^4} \left(\frac{\Delta m^2 + \kappa v_\Phi^2}{m_{DM}^2}\right)^2\right) \sqrt{1 - \frac{4m_Z^2}{s}}, \quad (29)$$

$$v_{rel}\sigma(D_{A_1}D_{A_1} \rightarrow q\bar{q}) = \frac{N_c \kappa^2 m_q^2}{16\pi} \frac{\sqrt{\left(1 - \frac{4m_f^2}{s}\right)^3}}{(s - m_{H_1}^2)^2 + m_{H_1}^2 \Gamma_{H_1}^2}, \quad (30)$$

$$v_{rel}\sigma(D_{A_1}D_{A_1} \rightarrow H_1 H_1) = \frac{\kappa^2}{64\pi s} \left(1 + \frac{3m_{H_1}^2}{s - m_{H_1}^2} - \frac{2\lambda v^2}{s - 2m_{H_1}^2}\right)^2 \sqrt{1 - \frac{4m_{H_1}^2}{s}}, \quad (31)$$

$$v_{rel}\sigma(D_{A_1}D_{A_1} \rightarrow \Xi_i \Xi_i) = \frac{\lambda_{11}^2}{64\pi s} \sqrt{1 - \frac{4m_{\Xi_i}^2}{s}}, \quad (32)$$

where $\kappa = \frac{\lambda_6 + \lambda_7}{4}$, $m_{DM} = m_{D_1}$, $\Delta m^2 = m_{D_{A_1}}^2 - m_{D_1}^2$, the mass splitting between the CP even and the odd parts of the neutral component of η , \sqrt{s} is the centre-of-mass energy, $N_c = 3$ stands for the color factor, $m_{H_1} = 125.7$ GeV and Γ_{H_1} is the total decay width of the SM Higgs boson which is equal to 4.1 MeV. Here, the final state represented as $\Xi_i \Xi_i$ stands for $\Xi_1^+ \Xi_1^-$, $\Xi_2^+ \Xi_2^-$, $\Xi_I^0 \Xi_I^0$, or $\Xi_R^0 \Xi_R^0$. From this, the dark matter relic abundance in the present Universe is estimated as follows (c.f. Ref. [37, 70]),

$$\Omega h^2 = \frac{0.1 \text{ pb}}{\langle \sigma v \rangle}, \quad \langle \sigma v \rangle = \frac{A}{n_{eq}^2}, \quad (33)$$

where $\langle \sigma v \rangle$ is the thermally averaged annihilation cross section, A is the total annihilation rate per unit volume at temperature T and n_{eq} is the equilibrium value of the particle density, which are given as [70],

$$A = \frac{T}{32\pi^4} \int_{4m_{D_{A_1}}^2}^{\infty} \sum_{p=W,Z,t,b,H_1,\Xi_i} g_p^2 \frac{s \sqrt{s - 4m_{D_{A_1}}^2}}{2} v_{rel}\sigma(D_{A_1}D_{A_1} \rightarrow SMSM) K_1\left(\frac{\sqrt{s}}{T}\right) ds, \\ n_{eq} = \frac{T}{2\pi^2} \sum_{p=W,Z,t,b,H_1,\Xi_i} g_p m_{D_{A_1}}^2 K_2\left(\frac{m_{D_{A_1}}}{T}\right) \quad (34)$$

with K_1 and K_2 being the modified Bessel functions of the second kind of order 1 and 2, respectively [70]. For the relic density calculation, we take $T = m_{A_1}/20$ as in Ref. [70], which corresponds to a typical freeze-out temperature. The DM relic density thus determined should match the required value as in Eqn. 27. In Fig. 7, we display the allowed parameter space (magenta points) in the $m_{DM} - \kappa$ plane that reproduces the correct dark matter relic abundance. In calculating the dark matter relic density, we have considered the annihilation of the DM into WW , ZZ , $H_1 H_1$, $t\bar{t}$, $b\bar{b}$,

and the components of the triplet scalar, which are the dominant channels. The masses of the charged and neutral components of Ξ are varied in the range 0.2-5 TeV and the quartic coupling λ_{11} is varied in the range $0 - 4\pi$. The pink band is disfavored by perturbativity whereas the gray shaded region is disfavored by the bounds from XENON1T [71]. The region above the blue line will be probed by the experiment DARWIN [72].

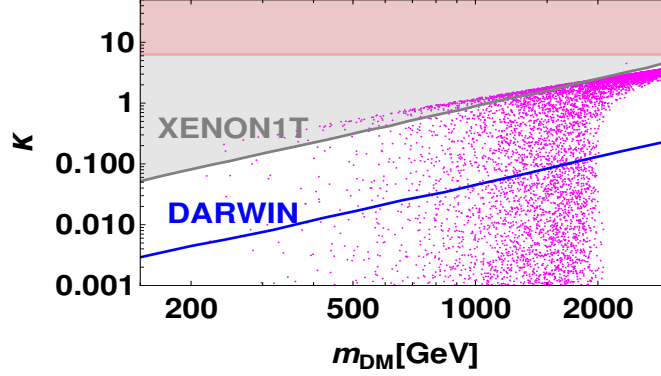


FIG. 7: Allowed $m_{DM} - \kappa$ region that reproduces the correct DM relic density (magenta points) for the scalar dark matter. Here, κ is the DM coupling to the SM Higgs boson. The pink band is disfavored by perturbativity. The gray region is excluded by XENON1T [71] while the blue line corresponds to the sensitivity of DARWIN [72].

C. Collider experiments

In this subsection we briefly discuss the collider signatures associated to the dark matter candidates in our model. Due to the remnant \mathcal{Z}_2 symmetry, the scalar and fermionic dark matter candidates will be produced in pairs. Because of the small mixing between η_R^0 and ξ_R^0 as well as η_I^0 and ξ_I^0 , we can take them approximately as the mass eigenstates. The neutral components of the dark doublet can be produced in pairs via the Drell-Yan mechanism mediated by the Z -boson or through vector boson fusion. This will correspond to a final state of 2 jets plus missing energy at the collider. Detailed studies of collider signatures arising from pair production of neutral components of the dark doublet via vector boson fusion are provided in [73].

Fig. 8 displays the total cross section for the pair production of η_R^0 and η_0^I via the Drell-Yan mechanism at a proton-proton collider for $\sqrt{s} = 14$ TeV (red line) and $\sqrt{s} = 100$ TeV (blue line) as a function of the CP-odd dark scalar mass $m_{D_{A1}}$, taken to vary in the range from 500 GeV up to 1.0 TeV. Here the mass of the CP even dark scalar, m_{D_1} has been set to be equal to 1 TeV. As shown in Figure 8, the total cross section for the CP-even and CP-odd dark scalar production at the LHC via the Drell-Yan mechanism reaches values of the order of 10^{-5} pb for $m_{D_{A1}}$ equals to 0.5 TeV, and decreases as $m_{D_{A1}}$ takes larger values.

The total Drell Yan production cross section increases by two orders of magnitude when one consider a 100 TeV proton-proton collider. In this case, the cross section reaches a value as high as 3×10^{-3} pb when the CP-odd dark scalar mass is set to 0.5 TeV. For the case of the fermionic DM candidate, the pair production of the charged components of the dark doublet through the Drell-Yan mechanism and their subsequent decays can give rise to a signature with opposite-sign dileptons plus missing energy in the final state. The observation of an excess of events of this opposite-sign dileptons final state configuration with respect to the SM background could provide support of this model at the LHC. A detailed study of collider signatures lies beyond the scope of the present work and will be taken up elsewhere.

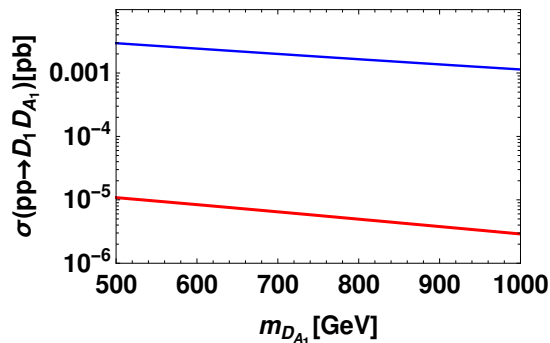


FIG. 8: Total cross section for the CP-even and CP-odd scalar dark-matter production via the Drell-Yan mechanism at a proton-proton collider for $\sqrt{s} = 14$ TeV (red line) and $\sqrt{s} = 100$ TeV (blue line) as a function of the CP-odd scalar dark matter mass $m_{D_{A_1}}$.

IV. SUMMARY AND CONCLUSIONS

In this work we have proposed a minimal model where neutrino mass generation arises at the one-loop level within the linear seesaw mechanism. Lepton number violation is seeded by a dark sector involving three Majorana fermions and two types of dark scalars, one isodoublet and the other isosinglet under the $SU(3)_c \otimes SU(2)_L \otimes U(1)_Y$ symmetry. The small neutrino masses arise from the spontaneous lepton number violation by a small Higgs triplet vacuum expectation value and involve the interplay of the one-loop dark sector seed with the linear seesaw mechanism. Our multiplet choice prevents the appearance of unwanted tree-level mass terms that could contribute to neutrino masses, making them genuinely calculable.

We have studied the predicted rates for charged lepton flavour violation, Figs. 2 and 3. We briefly discuss the prospects for testing our framework with the results of current and future lepton flavour violation searches. We have also commented on the WIMP dark-matter phenomenology of our model. For example, Figs. 4 and 5 correspond to the case where lightest dark fermion acts as the DM candidate. On the other hand, Figs. 6 and 7 are for the case in which the DM candidate is the lightest neutral scalar arising from the dark sector. Finally we make some comments on possible collider implications, Fig. 8. However, these would require a dedicated scrutiny outside the scope of this paper.

Note added

As this work was being completed we came to know that A. Batra, H. Camara and F. R. Joaquim have come up with an alternative realization of the same idea [74]. Prompted by a discussion with them, we noticed and corrected an inconsistency in the first version of our paper. We stress that, thanks to their different multiplet structures, the phenomenology of the two proposals is quite different.

ACKNOWLEDGMENTS

AECH has received funding from Chilean grants ANID-Chile FONDECYT 1210378, ANID PIA/APOYO AFB220004, ANID Programa Milenio code ICN2019_044. V.K.N. is supported by ANID-Chile Fondecyt Postdoctoral grant 3220005. The work of J.V. is supported by the Spanish grants PID2020-113775GB-I00 (AEI/10.13039/501100011033) and Prometeo CIPROM/2021/054 (Generalitat Valenciana).

-
- [1] A. B. McDonald, “Nobel Lecture: The Sudbury Neutrino Observatory: Observation of flavor change for solar neutrinos,” *Rev.Mod.Phys.* **88** (2016) 030502.
 - [2] T. Kajita, “Nobel Lecture: Discovery of atmospheric neutrino oscillations,” *Rev.Mod.Phys.* **88** (2016) 030501.
 - [3] G. Bertone, D. Hooper, and J. Silk, “Particle dark matter: Evidence, candidates and constraints,” *Phys.Rept.* **405** (2005) 279–390, [arXiv:hep-ph/0404175 \[hep-ph\]](#).
 - [4] J. Schechter and J. W. F. Valle, “Neutrino Masses in $SU(2) \times U(1)$ Theories,” *Phys.Rev.D* **22** (1980) 2227.
 - [5] J. Schechter and J. W. F. Valle, “Neutrino Decay and Spontaneous Violation of Lepton Number,” *Phys.Rev.D* **25** (1982) 774.
 - [6] E. Ma, “Radiative inverse seesaw mechanism for nonzero neutrino mass,” *Phys. Rev. D* **80** (2009) 013013, [arXiv:0904.4450 \[hep-ph\]](#).
 - [7] S. S. C. Law and K. L. McDonald, “Inverse seesaw and dark matter in models with exotic lepton triplets,” *Phys. Lett. B* **713** (2012) 490–494, [arXiv:1204.2529 \[hep-ph\]](#).
 - [8] A. Ahriche, S. M. Boucenna, and S. Nasri, “Dark Radiative Inverse Seesaw Mechanism,” *Phys. Rev. D* **93** no. 7, (2016) 075036, [arXiv:1601.04336 \[hep-ph\]](#).
 - [9] N. Rojas, R. Srivastava, and J. W. F. Valle, “Simplest Scoto-Seesaw Mechanism,” *Phys.Lett.B* **789** (2019) 132–136, [arXiv:1807.11447 \[hep-ph\]](#).
 - [10] S. Mandal, N. Rojas, R. Srivastava, and J. W. F. Valle, “Dark matter as the origin of neutrino mass in the inverse seesaw mechanism,” *Phys.Lett.B* **821** (2021) 136609, [arXiv:1907.07728 \[hep-ph\]](#).
 - [11] A. Abada, N. Bernal, A. E. C. Hernández, X. Marcano, and G. Piazza, “Gauged inverse seesaw from dark matter,” *Eur. Phys. J. C* **81** no. 8, (2021) 758, [arXiv:2107.02803 \[hep-ph\]](#).
 - [12] A. E. Cárcamo Hernández and S. F. King, “Littlest Inverse Seesaw Model,” *Nucl. Phys. B* **953** (2020) 114950, [arXiv:1903.02565 \[hep-ph\]](#).
 - [13] A. E. Cárcamo Hernández, L. T. Hue, S. Kovalenko, and H. N. Long, “An extended 3-3-1 model with two scalar triplets and linear seesaw mechanism,” *Eur. Phys. J. Plus* **136** no. 11, (2021) 1158, [arXiv:2001.01748 \[hep-ph\]](#).
 - [14] A. E. C. Hernández, H. N. Long, M. L. Mora-Urrutia, N. H. Thao, and V. V. Vien, “Fermion masses and mixings and $g - 2$ muon anomaly in a 3-3-1 model with D_4 family symmetry,” *Eur. Phys. J. C* **82** no. 8, (2022) 769, [arXiv:2104.04559 \[hep-ph\]](#).
 - [15] F. Bazzocchi, D. Cerdeno, C. Munoz, and J. W. F. Valle, “Calculable inverse-seesaw neutrino masses in supersymmetry,” *Phys.Rev.D* **81** (2010) 051701, [arXiv:0907.1262 \[hep-ph\]](#).
 - [16] A. E. Cárcamo Hernández, S. Kovalenko, J. W. F. Valle, and C. Vaquera-Araujo, “Predictive Pati-Salam theory of fermion masses and mixing,” *JHEP* **07** (2017) 118, [arXiv:1705.06320 \[hep-ph\]](#).
 - [17] A. E. Cárcamo Hernández and H. N. Long, “A highly predictive A_4 flavour 3-3-1 model with radiative inverse seesaw mechanism,” *J. Phys. G* **45** no. 4, (2018) 045001, [arXiv:1705.05246 \[hep-ph\]](#).
 - [18] A. E. Cárcamo Hernández, S. Kovalenko, J. W. F. Valle, and C. A. Vaquera-Araujo, “Neutrino predictions from a left-right symmetric flavored extension of the standard model,” *JHEP* **02** (2019) 065, [arXiv:1811.03018 \[hep-ph\]](#).
 - [19] A. E. Cárcamo Hernández, D. T. Huong, and H. N. Long, “Minimal model for the fermion flavor structure, mass hierarchy, dark matter, leptogenesis, and the electron and muon anomalous magnetic moments,” *Phys. Rev. D* **102** no. 5, (2020) 055002, [arXiv:1910.12877 \[hep-ph\]](#).
 - [20] A. E. Cárcamo Hernández, Y. Hidalgo Velásquez, and N. A. Pérez-Julve, “A 3-3-1 model with low scale seesaw mechanisms,” *Eur. Phys. J. C* **79** no. 10, (2019) 828, [arXiv:1905.02323 \[hep-ph\]](#).
 - [21] A. E. Cárcamo Hernández, J. Marchant González, and U. J. Saldaña Salazar, “Viable low-scale model with universal and inverse seesaw mechanisms,” *Phys. Rev. D* **100** no. 3, (2019) 035024, [arXiv:1904.09993 \[hep-ph\]](#).
 - [22] A. E. C. Hernández and I. Schmidt, “A renormalizable left-right symmetric model with low scale seesaw mechanisms,” *Nucl. Phys. B* **976** (2022) 115696, [arXiv:2101.02718 \[hep-ph\]](#).
 - [23] A. E. C. Hernández, D. T. Huong, and I. Schmidt, “Universal inverse seesaw mechanism as a source of the SM fermion mass hierarchy,” *Eur. Phys. J. C* **82** no. 1, (2022) 63, [arXiv:2109.12118 \[hep-ph\]](#).
 - [24] E. K. Akhmedov *et al.*, “Left-right symmetry breaking in NJL approach,” *Phys.Lett.B* **368** (1996) 270–280, [arXiv:hep-ph/9507275 \[hep-ph\]](#).

- [25] E. K. Akhmedov *et al.*, “Dynamical left-right symmetry breaking,” *Phys.Rev.D* **53** (1996) 2752–2780, [arXiv:hep-ph/9509255 \[hep-ph\]](#).
- [26] M. Malinsky, J. Romao, and J. W. F. Valle, “Novel supersymmetric SO(10) seesaw mechanism,” *Phys.Rev.Lett.* **95** (2005) 161801, [arXiv:hep-ph/0506296 \[hep-ph\]](#).
- [27] A. E. Cárcamo Hernández, S. Kovalenko, H. N. Long, and I. Schmidt, “A variant of 3-3-1 model for the generation of the SM fermion mass and mixing pattern,” *JHEP* **07** (2018) 144, [arXiv:1705.09169 \[hep-ph\]](#).
- [28] A. E. Cárcamo Hernández, N. A. Pérez-Julve, and Y. Hidalgo Velásquez, “Fermion masses and mixings and some phenomenological aspects of a 3-3-1 model with linear seesaw mechanism,” *Phys. Rev. D* **100** no. 9, (2019) 095025, [arXiv:1907.13083 \[hep-ph\]](#).
- [29] A. E. Cárcamo Hernández, S. Kovalenko, F. S. Queiroz, and Y. S. Villamizar, “An extended 3-3-1 model with radiative linear seesaw mechanism,” *Phys. Lett. B* **829** (2022) 137082, [arXiv:2105.01731 \[hep-ph\]](#).
- [30] R. Mohapatra and J. W. F. Valle, “Neutrino Mass and Baryon Number Nonconservation in Superstring Models,” *Phys.Rev.D* **34** (1986) 1642.
- [31] M. Gonzalez-Garcia and J. W. F. Valle, “Fast Decaying Neutrinos and Observable Flavor Violation in a New Class of Majoron Models,” *Phys.Lett.B* **216** (1989) 360–366.
- [32] A. Batra *et al.*, “Heavy neutrino signatures from leptophilic Higgs portal in the linear seesaw,” [arXiv:2304.06080 \[hep-ph\]](#).
- [33] A. Batra *et al.*, “Phenomenology of the simplest linear seesaw mechanism,” [arXiv:2305.00994 \[hep-ph\]](#).
- [34] G. Jungman, M. Kamionkowski, and K. Griest, “Supersymmetric dark matter,” *Phys.Rept.* **267** (1996) 195–373, [arXiv:hep-ph/9506380 \[hep-ph\]](#).
- [35] E. Ma, “Verifiable radiative seesaw mechanism of neutrino mass and dark matter,” *Phys.Rev.D* **73** (2006) 077301, [arXiv:hep-ph/0601225 \[hep-ph\]](#).
- [36] M. Hirsch *et al.*, “WIMP dark matter as radiative neutrino mass messenger,” *JHEP* **10** (2013) 149.
- [37] **Particle Data Group** Collaboration, R. Workman *et al.*, “Review of Particle Physics,” *PTEP* **2022** (2022) 083C01.
- [38] **ATLAS** Collaboration, G. Aad *et al.*, “Observation of a new particle in the search for the Standard Model Higgs boson with the ATLAS detector at the LHC,” *Phys.Lett.B* **716** (2012) 1–29, [arXiv:1207.7214 \[hep-ex\]](#).
- [39] **CMS** Collaboration, S. Chatrchyan *et al.*, “Observation of a New Boson at a Mass of 125 GeV with the CMS Experiment at the LHC,” *Phys.Lett.B* **716** (2012) 30–61, [arXiv:1207.7235 \[hep-ex\]](#).
- [40] Y. Chikashige, R. N. Mohapatra, and R. Peccei, “Are There Real Goldstone Bosons Associated with Broken Lepton Number?,” *Phys.Lett.B* **98** (1981) 265–268.
- [41] D. Fontes, J. C. Romao, and J. W. Valle, “Electroweak Breaking and Higgs Boson Profile in the Simplest Linear Seesaw Model,” *JHEP* **10** (2019) 245, [arXiv:1908.09587 \[hep-ph\]](#).
- [42] J. W. F. Valle, “Neutrinoless Double Beta Decay With Quasi Dirac Neutrinos,” *Phys.Rev.D* **27** (1983) 1672–1674.
- [43] G. Anamiati, M. Hirsch, and E. Nardi, “Quasi-Dirac neutrinos at the LHC,” *JHEP* **10** (2016) 010, [arXiv:1607.05641 \[hep-ph\]](#).
- [44] C. Arbeláez, C. Dib, K. Monsálvez-Pozo, and I. Schmidt, “Quasi-Dirac neutrinos in the linear seesaw model,” *JHEP* **07** (2021) 154, [arXiv:2104.08023 \[hep-ph\]](#).
- [45] J. Bernabeu *et al.*, “Lepton Flavor Nonconservation at High-Energies in a Superstring Inspired Standard Model,” *Phys.Lett.B* **187** (1987) 303–308.
- [46] P. Langacker and D. London, “Lepton Number Violation and Massless Nonorthogonal Neutrinos,” *Phys.Rev.D* **38** (1988) 907.
- [47] G. Branco, M. Rebelo, and J. W. F. Valle, “Leptonic CP Violation With Massless Neutrinos,” *Phys.Lett.B* **225** (1989) 385–392.
- [48] N. Rius and J. W. F. Valle, “Leptonic CP Violating Asymmetries in Z^0 Decays,” *Phys.Lett.B* **246** (1990) 249–255.
- [49] J. Casas and A. Ibarra, “Oscillating neutrinos and $\mu \rightarrow e, \gamma$,” *Nucl.Phys.B* **618** (2001) 171–204, [arXiv:hep-ph/0103065 \[hep-ph\]](#).
- [50] D. Forero, S. Morisi, M. Tortola, and J. W. F. Valle, “Lepton flavor violation and non-unitary lepton mixing in low-scale type-I seesaw,” *JHEP* **09** (2011) 142, [arXiv:1107.6009 \[hep-ph\]](#).
- [51] I. Cordero-Carrión, M. Hirsch, and A. Vicente, “General parametrization of Majorana neutrino mass models,” *Phys.Rev.D* **101** no. 7, (2020) 075032, [arXiv:1912.08858 \[hep-ph\]](#).
- [52] P. de Salas *et al.*, “2020 global reassessment of the neutrino oscillation picture,” *JHEP* **02** (2021) 071, [arXiv:2006.11237](#)

[hep-ph].

- [53] L. Lavoura, “General formulae for $f(1) \rightarrow f(2) + \gamma$,” *Eur. Phys. J. C* **29** (2003) 191–195, [arXiv:hep-ph/0302221](#).
- [54] L. T. Hue, L. D. Ninh, T. T. Thuc, and N. T. T. Dat, “Exact one-loop results for $l_i \rightarrow l_j \gamma$ in 3-3-1 models,” *Eur. Phys. J. C* **78** no. 2, (2018) 128, [arXiv:1708.09723 \[hep-ph\]](#).
- [55] MEG Collaboration, A. M. Baldini *et al.*, “Search for the lepton flavour violating decay $\mu^+ \rightarrow e^+ \gamma$ with the full dataset of the MEG experiment,” *Eur. Phys. J. C* **76** no. 8, (2016) 434, [arXiv:1605.05081 \[hep-ex\]](#).
- [56] A. M. Baldini *et al.*, “MEG Upgrade Proposal,” [arXiv:1301.7225 \[physics.ins-det\]](#).
- [57] MEG II Collaboration, M. Meucci, “MEG II experiment status and prospect,” *PoS NuFact2021* (2022) 120, [arXiv:2201.08200 \[hep-ex\]](#).
- [58] N. Bernal, A. E. Cárcamo Hernández, I. de Medeiros Varzielas, and S. Kovalenko, “Fermion masses and mixings and dark matter constraints in a model with radiative seesaw mechanism,” *JHEP* **05** (2018) 053, [arXiv:1712.02792 \[hep-ph\]](#).
- [59] Planck Collaboration, N. Aghanim *et al.*, “Planck 2018 results. VI. Cosmological parameters,” *Astron. Astrophys.* **641** (2020) A6, [arXiv:1807.06209 \[astro-ph.CO\]](#).
- [60] L. Lopez Honorez, E. Nezri, J. F. Oliver, and M. H. G. Tytgat, “The Inert Doublet Model: An Archetype for Dark Matter,” *JCAP* **02** (2007) 028, [arXiv:hep-ph/0612275](#).
- [61] D. Restrepo and A. Rivera, “Phenomenological consistency of the singlet-triplet scotogenic model,” *JHEP* **04** (2020) 134, [arXiv:1907.11938 \[hep-ph\]](#).
- [62] I. M. Ávila, V. De Romeri, L. Duarte, and J. W. F. Valle, “Phenomenology of scotogenic scalar dark matter,” *Eur. Phys. J. C* **80** (2020) 908, [arXiv:1910.08422 \[hep-ph\]](#).
- [63] S. K. Kang *et al.*, “Scotogenic dark matter stability from gauged matter parity,” *Phys. Lett. B* **798** (2019) 135013, [arXiv:1902.05966 \[hep-ph\]](#).
- [64] A. E. Cárcamo Hernández, J. W. F. Valle, and C. A. Vaquera-Araujo, “Simple theory for scotogenic dark matter with residual matter-parity,” *Phys. Lett. B* **809** (2020) 135757, [arXiv:2006.06009 \[hep-ph\]](#).
- [65] A. E. C. Hernández, C. Hati, S. Kovalenko, J. W. F. Valle, and C. A. Vaquera-Araujo, “Scotogenic neutrino masses with gauged matter parity and gauge coupling unification,” *JHEP* **03** (2022) 034, [arXiv:2109.05029 \[hep-ph\]](#).
- [66] A. E. C. Hernández, S. Kovalenko, M. Maniatis, and I. Schmidt, “Fermion mass hierarchy and $g - 2$ anomalies in an extended 3HDM Model,” *JHEP* **10** (2021) 036, [arXiv:2104.07047 \[hep-ph\]](#).
- [67] A. E. Cárcamo Hernández, C. Espinoza, J. C. Gómez-Izquierdo, J. M. González, and M. Mondragón, “Predictive extended 3HDM with S_4 family symmetry,” [arXiv:2212.12000 \[hep-ph\]](#).
- [68] T. Hambye, F. S. Ling, L. Lopez Honorez, and J. Rocher, “Scalar Multiplet Dark Matter,” *JHEP* **07** (2009) 090, [arXiv:0903.4010 \[hep-ph\]](#). [Erratum: JHEP 05, 066 (2010)].
- [69] S. Bhattacharya, P. Poulose, and P. Ghosh, “Multipartite Interacting Scalar Dark Matter in the light of updated LUX data,” *JCAP* **04** (2017) 043, [arXiv:1607.08461 \[hep-ph\]](#).
- [70] J. Edsjo and P. Gondolo, “Neutralino relic density including coannihilations,” *Phys. Rev. D* **56** (1997) 1879–1894, [arXiv:hep-ph/9704361](#).
- [71] XENON Collaboration, E. Aprile *et al.*, “Dark Matter Search Results from a One Ton-Year Exposure of XENON1T,” *Phys. Rev. Lett.* **121** no. 11, (2018) 111302, [arXiv:1805.12562 \[astro-ph.CO\]](#).
- [72] DARWIN Collaboration, J. Aalbers *et al.*, “DARWIN: towards the ultimate dark matter detector,” *JCAP* **11** (2016) 017, [arXiv:1606.07001 \[astro-ph.IM\]](#).
- [73] B. Dutta, G. Palacio, J. D. Ruiz-Alvarez, and D. Restrepo, “Vector Boson Fusion in the Inert Doublet Model,” *Phys. Rev. D* **97** no. 5, (2018) 055045, [arXiv:1709.09796 \[hep-ph\]](#).
- [74] A. Batra, H. Câmara, and F. Joaquim, “Dark linear seesaw mechanism,” [arXiv:2305.01687 \[hep-ph\]](#).